Angular analysis of the decay $B \to K^* l^+ l^-$ at the Belle experiment

Leonard Koch

Justus Liebig Universität Gießen, II physikalisches Institut

(Dated: September 11, 2014)

This report describes my project within the Desy Summer Student Programme 2014 in the Belle group. I implemented a fit to angular distributions in the decay $B \to K^*(\to K\pi)l^+l^-$ to extract parameters that might be sensitive to physics beyond the Standard Model. I performed a Monte Carlo toy study in order to test four different realisations of the fit. Althought the Belle experiment has rather limited statistics, it is sufficient to make a significant measurement of these parameters.

I. INTRODUCTION

The $b \to sl^+l^-$ process in $B \to K^*(\to K\pi)l^+l^-$, where l stands for e or μ, is a flavor changing neutral current which is forbidden in the Standard Model (SM) at tree level and can occur at lowest order in electroweak penguin and box diagrams (see Figure 1). The angular distribution of the $K\pi l^+l^-$ final state is sensitive to physics beyond the SM that could contribute to these diagrams. The decay has been studied extensively by Belle [2], BaBar [2], CDF [3], and LHCb [4] and the results on various observables have been found to be in agreement with the SM. Last year LHCb published a measurement of observables in the angular distribution of this decay and found a $3.7\,\sigma$ descrepancy to the SM prediction for P_5' (definition see section III Eq. 1 and 2) in one dimuon invariant mass squared bin of $4.30\,\mathrm{GeV}^2/c^4$ - $8.68\,\mathrm{GeV}^2/c^4$ [5]. To clarify the nature of this discrepancy, a second independent measurement is needed. In this report the first stage of a study is presented to evaluate the sensitivity of the Belle experiment to the same observables as measured by LHCb.

The next section is a brief description of the Belle detector. In Section III the kinematic variables and the differential decay rate together with an angle transformation is presented. The different fitting techniques and the Monte Carlo (MC) toy study is explained and its result is shown in Section IV. Conclusions and a short outlook can be found in Section V.

II. THE BELLE DETECTOR

The Belle detector collected $\sim 1000\,\mathrm{fb}^{-1}$ of data at the asymmetric e^+e^- collider KEK-B operating at the $\Upsilon(nS)$ resonances at KEK in Tsukuba, Japan. It is a multipurpose large-solid-angle megnetic spectrometer designed to measure time dependent CP violation in B meson decays. It covers a polar angle between 17° and 150° and has the typical 'onion skin' layout.

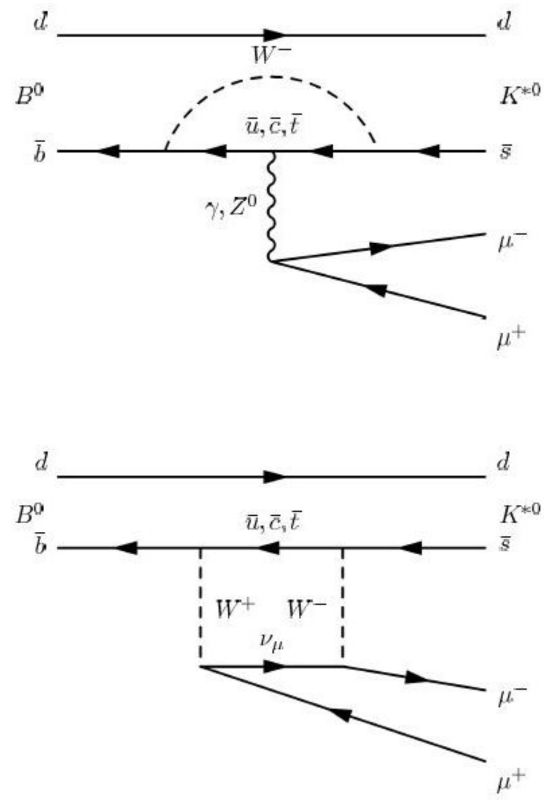

FIG. 1. Above: One possible electroweak penguin diagram for the process $B^0 \to K^{*0}\mu^+\mu^-$. Below: A box diagram for the same process [1].

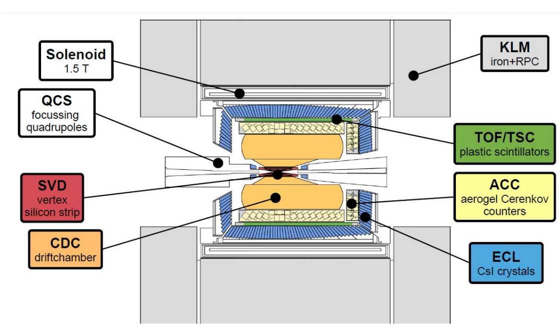

FIG. 2. Schematic view of the Belle detector, courtesy of Torben Ferber.

The central part of the detector is a multilayer double sided silicon strip detector surounding the beryllium beam pipe for precise vertex reconstruction. Tracking of charged particles is per-

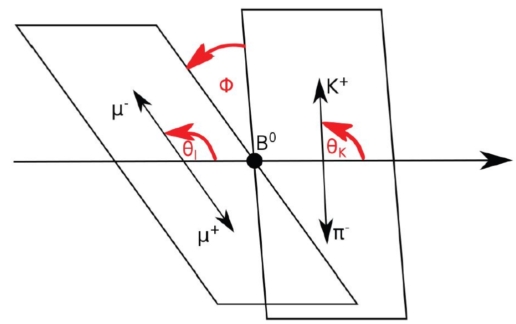

FIG. 3. Definitions of the angles in $B \to K^* l^+ l^-$ [1].

formed by a central drift chamber (CDC). Particle identification is provided by aerogel threshold Cherenkov counters, time-of-flight plastic scintillators and the dE/dx information from the CDC. Eletromagentic showers are reconstructed in the $CsI(Tl)$ calorimeter inside the 1.5 T superconducting solenoid coil. The iron flux return is used to detect K_L mesons und muons (see Figure 2). A detailed description of the detector can be found elsewhere [6].

III. THE PROBABILITY DENSITY FUNCTION (PDF)

A. Definition of kinematic variables

The angular distribution of the decay $B^0 \to K^{*0}(\to K^+\pi^-)l^+l^-$ where l denotes either e or μ can be described by four kinematic variables: q^2 is the squared invariant mass of the dilepton system, θ_K is the angle between the direction of the kaon and the opposite direction of the B^0 ($\overline{B}^0$) in the K^{*0} ($\overline{K}^{*0}$) rest frame, θ_l is the angle between the direction of the l^+ (l^-) and the opposite direction of the B^0 ($\overline{B}^0$) in the dilepton rest frame, and the angle ϕ is defined as the angle between the K^{*0} ($\overline{K}^{*0}$) decay plane and the dilepton decay plane in the B^0 ($\overline{B}^0$) meson rest frame (see Figure 3). A more formal definition of the angles can be found in Ref. [7].

B. The differential decay rate

Using the definitions of Ref. [8], neglecting the lepton masses and summing over B^0 and $\overline{B}^0$ decays, the differential decay rate can be expressed as

$$\begin{aligned}\frac{1}{\mathrm{d}\Gamma/\mathrm{d}q^2}\frac{\mathrm{d}\Gamma}{\mathrm{d}q^2\mathrm{d}\cos\theta_K\mathrm{d}\cos\theta_l\mathrm{d}\phi} =&\frac{9}{32\pi}\Bigg[\frac{3}{4}(1-F_L)\sin^2\theta_K + F_L\cos^2\theta_K \\ &+\frac{1}{4}(1-F_L)\sin^2\theta_K\cos 2\theta_l - F_L\cos^2\theta_K\cos 2\theta_l \\ &+ S_3\sin^2\theta_K\sin^2\theta_l\cos 2\phi + S_4\sin 2\theta_K\sin 2\theta_l\cos\phi \\ &+ S_5\sin 2\theta_K\sin 2\theta_l\cos\phi + S_6\sin^2\theta_K\cos\theta_l \\ &+ S_7\sin 2\theta_K\sin\theta_l\sin\phi + S_8\sin 2\theta_K\sin 2\theta_l\sin\phi \\ &+ S_9\sin^2\theta_K\sin^2\theta_l\sin 2\phi \Bigg],\end{aligned} \tag{1}$$

with F_L and S_i being q^2 dependent and sensitive to new physics. The observables

$$P'_{4,5,6,8} = \frac{S_{4,5,7,8}}{\sqrt{F_L(1-F_L)}} \tag{2}$$

are regarded as largely independent of form factor uncertainties [9].

We assume that the pdf defined in Eq. 1 is also valid for charged B meson decays.

C. Binning in q^2 and transformation of the angles

Due to the q^2 dependence of the observables in the angular distribution the fit is performed in six q^2 bins (see Table I). The gaps between $8.68\,\mathrm{GeV}^2/c^4$ - $10.09\,\mathrm{GeV}^2/c^4$ and $10.90\,\mathrm{GeV}^2/c^4$ - $14.18\,\mathrm{GeV}^2/c^4$ are vetos for background from $B^0 \to K^{*0}J/\psi(\to l^+l^-)$ and $B^0 \to K^{*0}\psi(2S)(\to l^+l^-)$.

The most straight forward way in order to extract the observables P'_4, P'_5, P'_6 and P'_8 would be to fit the pdf defined in Eq. 1 to the angular distribution measured in an experiment. Such a fit is expected to be very unstable if statistics is limited because of the large number of free parameters in the fit. To reduce the number of parameters per fit, the angles are transformed in one of the following manners:

$$P'_4\,/\,S_4\;:\begin{cases}\phi\to-\phi & \text{for}\,\phi<0\\ \phi\to\pi-\phi & \text{for}\,\theta_l>\pi/2\\ \theta_l\to\pi-\theta_l & \text{for}\,\theta_l>\pi/2,\end{cases} \tag{3}$$

$$P_5' \,/\, S_5 \; : \begin{cases} \phi \to -\phi & \text{for}\, \phi < 0 \\ \theta_l \to \pi - \theta_l & \text{for}\, \theta_l > \pi/2, \end{cases} \quad (4)$$

$$P_6' \,/\, S_7 \; : \begin{cases} \phi \to \pi - \phi & \text{for}\, \phi > \pi/2 \\ \phi \to -\pi - \phi & \text{for}\, \phi < -\pi/2 \\ \theta_l \to \pi - \theta_l & \text{for}\, \theta_l > \pi/2, \end{cases} \quad (5)$$

$$P_8' \,/\, S_8 \; : \begin{cases} \phi \to \pi - \phi & \text{for}\, \phi > \pi/2 \\ \phi \to -\pi - \phi & \text{for}\, \phi < -\pi/2 \\ \theta_K \to \pi - \theta_K & \text{for}\, \theta_l > \pi/2 \\ \theta_l \to \pi - \theta_l & \text{for}\, \theta_l > \pi/2. \end{cases} \quad (6)$$

These transformations exploit the symmetries of the angular terms in Eq. 1, so that only the first five terms and one of the terms containing the P_i' survive. One gets four datasets and four pdfs, each containing only three parameters: F_L, S_3 and one of the P_i'. These angular transformations were also done in the analysis described in Ref. [5].

IV. MONTE CARLO TOY STUDY

A. Estimation of the number of signal events

For the MC study it is important to know, how many signal events are expected. For this aim a large MC data sample of $B \to K^* l^+ l^-$ was generated, propagated through the detector and reconstructed [10]. The numbers of events per q^2 bin were scaled down so that the total number of events is 300, which is reasonable if we sum over neutral and charged B mseons. The expected numbers of signal events per bin are listed in Table I.

TABLE I. Dividing the data into bins of q^2. Additionally the expected number of events per bin is given for the case of 300 signal events in all bins together.

bin	q^2 [GeV$^2/c^4$]	expected number of signal events
1	0.10 − 2.00	59
2	2.00 − 4.30	37
3	4.30 − 8.68	77
4	10.09 − 12.90	59
5	14.18 − 16.00	34
6	16.00 − 19.00	34

B. Fitting techniques

I always performed an unbinned maximum likelihood fit using RooFit [11]. After every fit asymmetric errors are calculated. These are then refered to as the upper and the lower error.

Four different possibilities of performing the fit were considered: One can fit the pdfs to the distributions in $\cos\theta_l$, $\cos\theta_K$ and ϕ or one can fit the pdfs to the distributions in θ_l, θ_K and ϕ. The latter requires the transformation

$$\frac{\mathrm{d}\Gamma}{\mathrm{d}\theta_l \mathrm{d}\theta_K \mathrm{d}\phi} = \frac{\mathrm{d}\Gamma}{\mathrm{d}\cos\theta_l \mathrm{d}\cos\theta_K \mathrm{d}\phi} \times \sin\theta_l \sin\theta_K. \quad (7)$$

Additionally, one can perform the fit for each of the four datasets and pdfs independently or simultaniously in a combined fit since all four pdfs share two common parameters: F_L and S_3.

C. Procedure of the Monte Carlo toy study

One major part of my project was to evaluate how sensitive this fit is to the observables defined in Eq. 2, i.e. how large the errors of these observables are. Therefore, 10 000 data samples with the number of entries given in Table I are generated according to the 'untransformed' pdf defined in Eq. 1. For the generation, the parameters F_L, S_3, P_4', P_5', P_6' are fixed to SM predictions from Ref. [9], whereas P_8' is fixed to the measurement by LHCb [5] and S_6 and S_9 are chosen such that the pdf stays not negative in the allowed range of the angles. Then these data samples are transformed as described in (3) - (6). The next step is to perform each of the four fits to every of the 10 000 data samples and to store the fitted values and the asymmetric errors of the values. The mean values of the resulting distributions of the errors are regarded as good measures for the errors of the fit to data. A pull can be defined as

$$pull_{value} = \frac{value_{fitted} - value_{true}}{error_{value}}. \qquad (8)$$

If $value_{fitted} - value_{true} > 0$ then the magnitude of the lower error will be asigned. Otherwise the upper error will be asigned. With this definition it is easy to see that a perfect pull distribution should have a mean of zero and a standard deviation of one. Therefore, the mean and the standard deviation of the pull distribution is a measure for the quality of the fitting technique.

D. Results

The results of this study are presented in Tables II and III. The mean value of the error for all observables P_i' is approximately the same and is independent of the fitting technique. As expected, the absolute value of the mean error is close to an antiproportional behavior compared to the number of generated events per bin (see Table I). Figures 4 and 5 show the mean value of the fit error of P_4' and P_5'.

The pull distributions for P_6' and P_8' are almost perfect. The deviations from the ideal values are always less than 0.15. For P_4' and P_5' the pull distributions show a larger deviation from the ideal values (up to 0.5). To be sure that this is not caused by a bug in the MC toy study, it is repeated: once 100 events are generated in each bin and a second time 1000 events are generated per bin. In Figures 6 and 7 the result is shown for P_5'. One can see that with increasing statistics the pull distributions improve. This behavior is also found for P_4'. The outcome of this additional study is that the deviation of the pull distribution from the ideal one is related to the low statistics.

In Figures 8 and 9 the expected sensitivity to the parameters P_4' and P_5' in comparison to the LHCb measurement [5] is shown.

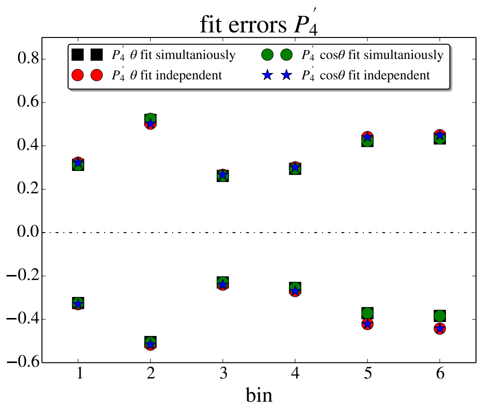

FIG. 4. The mean value of the asymmetric error of the parameter P_4' for all four fitting techniques in the six q^2 bins. The positive value is the upper error and the negative is the lower error.

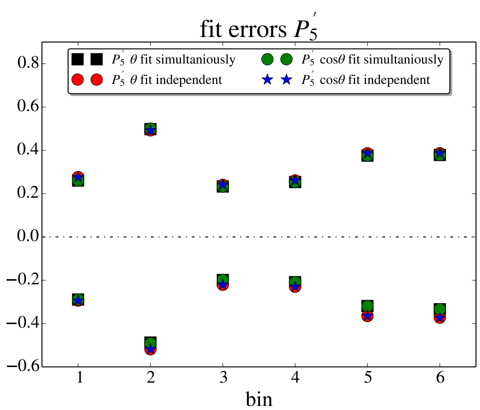

FIG. 5. The mean value of the asymmetric error of the parameter P_5' for all four fitting techniques in the six q^2 bins. The positive value is the upper error and the negative is the lower error.

V. CONCLUSION AND OUTLOOK

Although LHCb has higher statistics than Belle ($\sim$ 880 signal events [7]), this study has shown that the sensitivity of Belle is sufficient to make a significant independent measurement of the observables $P'_{4,5,6,8}$. Nevertheless, this is only the first stage of the whole sensitivity study, since background and efficiency corrections need to be included in the pdf to get a more realistic picture.

In the near future, LHCb will analyze more data which will clear up the behavior of the measured $3.7\,\sigma$ effect. Also Belle II will start operating in the next years to provide a second measurement with higher statistics.

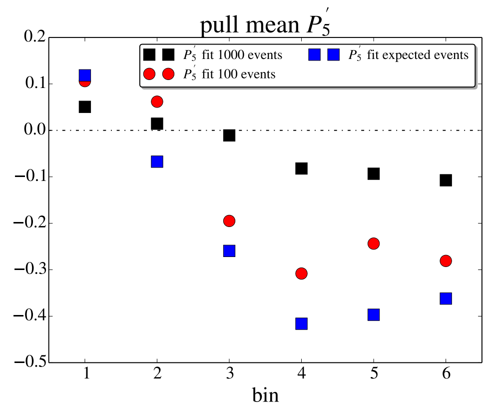

FIG. 6. The mean value of the pull distribution for the parameter P_5' for three different numbers of generated events in the six q^2 bins.

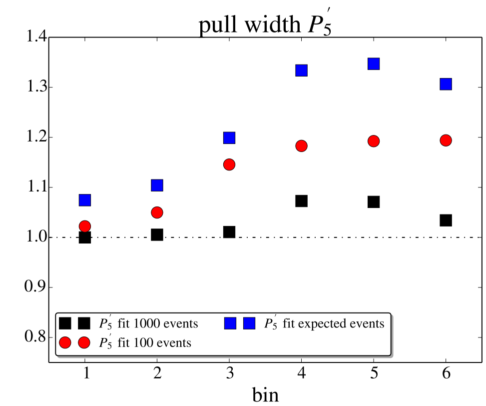

FIG. 7. The RMS value of the pull distribution for the parameter P_5' for three different numbers of generated events in the six q^2 bins.

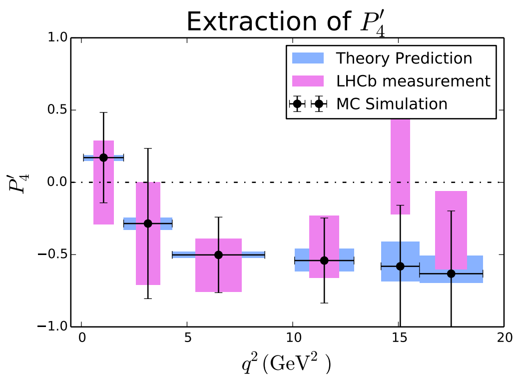

FIG. 8. The expected statistical error for the fit of the parameter P'_4 (MC Simulation) in comparison to the measurement of LHCb [5] (including systematic uncertainties) and SM predictions [9].

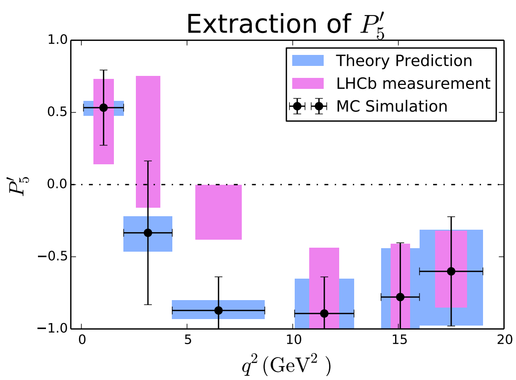

FIG. 9. The expected statistical error for the fit of the parameter P'_5 (MC Simulation) in comparison to the measurement of LHCb [5] (including systematic uncertainties) and SM predictions [9].

ACKNOWLEDGMENTS

I want to thank the Helmholtz Association, Desy, Belle, and especially the Desy Belle group to give me the opportunity to participate in this program and to be part of state-of-the-art research. A big thank you goes to the organization team of the Summer Student Programme. From the Belle group at Desy, I want to mention the names of Oliver Frost, Sergey Yashchenko and the one who deserves the most acknowledgments, Simon Wehle.

[1] M. D. Cian, *Track Reconstruction Efficiency and Analysis of* $B^0 \to K^{*0}\mu^+\mu^-$ *at the LHCb Experiment*, Ph.D. thesis, Universität Zürich (2013).

[2] A. J. Bevan *et al.*, "The physics of the b factories," (2014), arXiv:1406.6311.

[3] T. Aaltonen *et al.* (CDF Collaboration), Phys. Rev. Lett. **108**, 081807 (2012).

[4] R. Aaij *et al.* (LHCb Collaboration), Phys. Rev. Lett. **108**, 181806 (2012).

[5] R. Aaij *et al.* (LHCb Collaboration), Phys. Rev. Lett. **111**, 191801 (2013).

[6] A. Abashian *et al.*, Nuclear Instruments and Methods in Physics Research Section A: Accelerators, Spectrometers, Detectors and Associated Equipment **479**, 117 (2002), detectors for Asymmetric B-factories.

[7] R. Aaij *et al.*, Journal of High Energy Physics **2013**, 131 (2013), 10.1007/JHEP08(2013)131.

[8] W. Altmannshofer *et al.*, Journal of High Energy Physics **2009**, 019 (2009).

[9] S. Descotes-Genon, T. Hurth, J. Matias, and J. Virto, Journal of High Energy Physics **2013**, 137 (2013), 10.1007/JHEP05(2013)137.

[10] S. Wehle, (2014), private communication.

[11] W. Verkerke and D. Kirkby, "The roofit toolkit for data modeling," (2003), arXiv:physics/0306116.

TABLE II. Mean values of the upper and lower fit errors for the paramters P'_i for the four fitting techniques.

P'_4 fit	simultanious, θ		independent, θ		simultanious, $\cos\theta$		independent, $\cos\theta$	
bin	upper	lower	upper	lower	upper	lower	upper	lower
1	0.313	-0.325	0.322	-0.330	0.313	-0.325	0.322	-0.330
2	0.520	-0.505	0.502	-0.517	0.525	-0.507	0.502	-0.516
3	0.261	-0.230	0.266	-0.240	0.261	-0.230	0.266	-0.240
4	0.294	-0.255	0.301	-0.270	0.294	-0.255	0.301	-0.270
5	0.422	-0.372	0.440	-0.422	0.422	-0.372	0.440	-0.422
6	0.434	-0.384	0.449	-0.443	0.434	-0.384	0.449	-0.443

P'_5 fit	simultanious, θ		independent, θ		simultanious, $\cos\theta$		independent, $\cos\theta$	
bin	upper	lower	upper	lower	upper	lower	upper	lower
1	0.260	-0.289	0.276	-0.294	0.260	-0.289	0.276	-0.294
2	0.498	-0.487	0.492	-0.519	0.500	-0.491	0.492	-0.519
3	0.233	-0.199	0.241	-0.221	0.233	-0.199	0.241	-0.221
4	0.254	-0.209	0.261	-0.230	0.254	-0.209	0.261	-0.230
5	0.376	-0.319	0.387	-0.365	0.376	-0.319	0.386	-0.365
6	0.379	-0.334	0.387	-0.373	0.379	-0.334	0.387	-0.373

P'_6 fit	simultanious, θ		independent, θ		simultanious, $\cos\theta$		independent, $\cos\theta$	
bin	upper	lower	upper	lower	upper	lower	upper	lower
1	0.295	-0.290	0.299	-0.297	0.295	-0.290	0.299	-0.297
2	0.496	-0.494	0.501	-0.507	0.501	-0.497	0.500	-0.507
3	0.261	-0.260	0.264	-0.263	0.261	-0.260	0.264	-0.263
4	0.285	-0.285	0.289	-0.288	0.285	-0.285	0.289	-0.288
5	0.388	-0.388	0.400	-0.400	0.388	-0.388	0.400	-0.400
6	0.400	-0.401	0.414	-0.414	0.400	-0.401	0.414	-0.414

P'_8 fit	simultanious, θ		independent, θ		simultanious, $\cos\theta$		independent, $\cos\theta$	
bin	upper	lower	upper	lower	upper	lower	upper	lower
1	0.322	-0.318	0.328	-0.325	0.322	-0.318	0.328	-0.325
2	0.509	-0.506	0.502	-0.508	0.515	-0.509	0.501	-0.507
3	0.268	-0.265	0.270	-0.267	0.268	-0.265	0.270	-0.267
4	0.303	-0.298	0.305	-0.301	0.303	-0.298	0.305	-0.301
5	0.421	-0.419	0.434	-0.433	0.421	-0.419	0.434	-0.433
6	0.434	-0.439	0.449	-0.453	0.434	-0.439	0.449	-0.453

TABLE III. Mean values and standard deviation (RMS) of the pull distributions for the paramters P_i' for the four fitting techniques.

P_4' fit	simultanious, θ		independent, θ		simultanious, $\cos\theta$		independent, $\cos\theta$	
bin	mean	RMS	mean	RMS	mean	RMS	mean	RMS
1.	0.027	1.055	0.033	1.057	0.027	1.055	0.033	1.057
2.	-0.071	1.157	-0.049	1.105	-0.070	1.157	-0.049	1.105
3.	-0.075	1.096	-0.108	1.090	-0.075	1.096	-0.108	1.090
4.	-0.115	1.168	-0.151	1.156	-0.115	1.168	-0.151	1.156
5.	-0.199	1.295	-0.226	1.236	-0.199	1.295	-0.226	1.236
6.	-0.276	1.379	-0.296	1.296	-0.276	1.379	-0.296	1.296

P_5' fit	simultanious, θ		independent, θ		simultanious, $\cos\theta$		independent, $\cos\theta$	
bin	mean	RMS	mean	RMS	mean	RMS	mean	RMS
1.	0.079	1.081	0.118	1.074	0.079	1.081	0.118	1.074
2.	-0.053	1.112	-0.067	1.104	-0.053	1.112	-0.067	1.104
3.	-0.162	1.243	-0.259	1.199	-0.162	1.243	-0.260	1.199
4.	-0.300	1.347	-0.416	1.334	-0.300	1.347	-0.416	1.334
5.	-0.338	1.425	-0.397	1.347	-0.338	1.425	-0.396	1.347
6.	-0.298	1.342	-0.362	1.306	-0.298	1.342	-0.362	1.306

P_6' fit	simultanious, θ		independent, θ		simultanious, $\cos\theta$		independent, $\cos\theta$	
bin	mean	RMS	mean	RMS	mean	RMS	mean	RMS
1.	-0.021	1.049	-0.026	1.058	-0.021	1.049	-0.026	1.058
2.	0.000	1.081	-0.002	1.089	-0.002	1.080	-0.002	1.089
3.	-0.013	1.031	-0.016	1.040	-0.013	1.031	-0.016	1.040
4.	-0.011	1.042	-0.010	1.053	-0.011	1.042	-0.010	1.053
5.	0.001	1.074	-0.001	1.080	0.001	1.074	-0.001	1.080
6.	0.008	1.056	0.006	1.060	0.008	1.056	0.006	1.060

P_8' fit	simultanious, θ		independent, θ		simultanious, $\cos\theta$		independent, $\cos\theta$	
bin	mean	RMS	mean	RMS	mean	RMS	mean	RMS
1.	-0.028	1.045	-0.030	1.047	-0.028	1.045	-0.030	1.047
2.	-0.019	1.134	-0.006	1.105	-0.020	1.134	-0.006	1.105
3.	-0.005	1.046	-0.007	1.051	-0.005	1.046	-0.007	1.051
4.	-0.039	1.051	-0.041	1.056	-0.039	1.051	-0.041	1.056
5.	-0.013	1.085	-0.017	1.083	-0.013	1.085	-0.017	1.083
6.	0.026	1.072	0.029	1.068	0.026	1.072	0.029	1.068